

Imaging Stars with Quantum Error Correction

Zixin Huang^{1,*}, Gavin K. Brennen^{1,†}, and Yingkai Ouyang^{2,3,‡}

¹Centre for Engineered Quantum Systems, School of Mathematical and Physical Sciences, Macquarie University, NSW 2109, Australia

²Department of Electrical and Computer Engineering, National University of Singapore, Singapore

³Centre of Quantum Technologies, National University of Singapore, Singapore

 (Received 6 May 2022; accepted 21 October 2022; published 16 November 2022)

The development of high-resolution, large-baseline optical interferometers would revolutionize astronomical imaging. However, classical techniques are hindered by physical limitations including loss, noise, and the fact that the received light is generally quantum in nature. We show how to overcome these issues using quantum communication techniques. We present a general framework for using quantum error correction codes for protecting and imaging starlight received at distant telescope sites. In our scheme, the quantum state of light is coherently captured into a nonradiative atomic state via stimulated Raman adiabatic passage, which is then imprinted into a quantum error correction code. The code protects the signal during subsequent potentially noisy operations necessary to extract the image parameters. We show that even a small quantum error correction code can offer significant protection against noise. For large codes, we find noise thresholds below which the information can be preserved. Our scheme represents an application for near-term quantum devices that can increase imaging resolution beyond what is feasible using classical techniques.

DOI: [10.1103/PhysRevLett.129.210502](https://doi.org/10.1103/PhysRevLett.129.210502)

The performance of an imaging system is limited by diffraction: the resolution is proportional to its aperture and inversely proportional to the wavelength λ . Together these place a fundamental limit on how well one can image the objects of interest. Typical techniques employed to enable quantum sensing and quantum imaging to surpass classical limits utilize entanglement [1,2], source engineering [3], or squeezing [4] to suppress intensity fluctuations. These techniques require manipulating the objects or illuminating them with light that has special properties. However, often it is the case, e.g., for astronomy, we cannot illuminate the objects of interest. Rather, all we can do is analyze the light that reaches us.

Several challenges hinder the progress in building large-baseline optical interferometers, one of which is the presence of noise and transmission loss that ultimately limits the distance between telescope sites. Quantum technologies can help bypass transmission losses: using quantum memories and entanglement, we can replace the direct optical links, allowing us to go to large distances. In the most direct approach [5], we could store the signal into atomic states and perform operations to extract the information; however, such states are sensitive to optical decay and other decoherences. One way to combat noise is to employ quantum error correction (QEC). QEC has been predominantly studied in the context of quantum computation [6] and specialized sensing protocols [7–16].

In this Letter, we produce a general framework for using QEC codes to protect the information in the received light. This is the first time that QEC has been applied to a

quantum parameter estimation task where the probe state need not be prepared by the experimenter. We eliminate optical decay in quantum memories by coupling light into nonradiative atomic qubit states via the well-developed process known as stimulated Raman adiabatic passage (STIRAP) [17]. Our scheme can also accommodate for multiphoton events. Two general proof-of-principle results [5,18] have investigated the potential for entanglement-aided imaging, when the quantum memories and subsequent operations are ideal. Here, we take into account noise sources and propose a robust encoding of the signal into quantum memories. Any imaging task can be translated into a parameter estimation task, where the quantity of interest is the quantum Fisher information (QFI). We show that even a small QEC code can offer significant protection against noise which degrades resolution.

The protocol.—We show an overview of our protocol in Fig. 1. Consider a two-site scenario (Alice and Bob), each holding a telescope station and they are separated by large distances. The layer of quantum technology is schematically shown in panel (i), where light from astronomical sources is collected: Alice and Bob share predistributed entanglement, and the sites each contain quantum memories into which the light is captured. This becomes the encoder operation in (ii): they each prepare (locally) their set of qubits into some QEC code. The received state ρ_* is imprinted onto the code via an encoder, resulting in the logical state ρ_{AB} shared between Alice and Bob. The state is thus protected from subsequent noisy operations. Panel (iii) shows the circuit of the encoder.

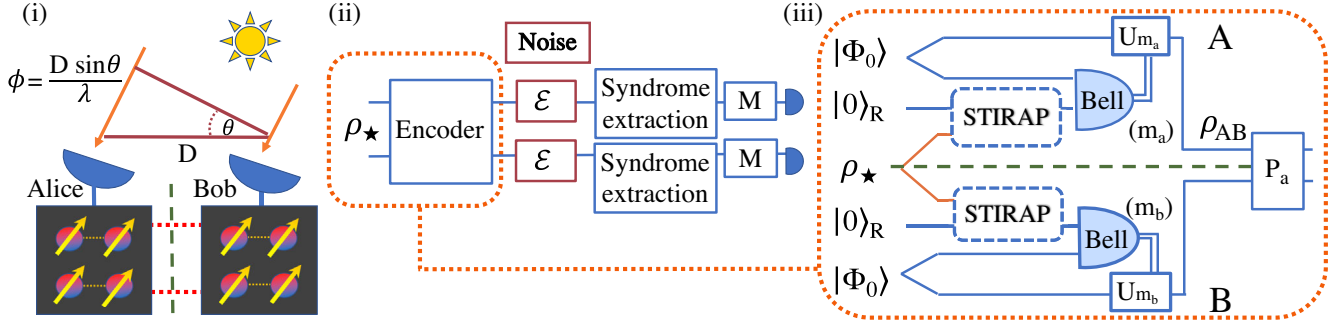


FIG. 1. Overview of our protocol. (i) Light at wavelength λ is collected at two sites (Alice and Bob) separated by distance D , each holding quantum memories and sharing Bell pairs. (ii) A general framework for the process of encoding, error correction, and measuring the signal. The starlight ρ_\star is input into the encoder, which outputs a logical state of a quantum code. The memory qubits and subsequent operations are potentially noisy as modeled by local channels \mathcal{E} . Any correctible error is detected by syndrome measurements and the final step is a local Clifford measurement M , which depends on the error syndromes, and extracts the parameters of interest from the state. (iii) A detailed schematic showing how to encode the starlight into a logical state. The green dashed line denotes the spatial separation between Alice and Bob. U_m are Pauli corrections depending on the outcome of local Bell measurements. P_a is a parity measurement to project out the vacuum component (and multiphoton contributions) and is the only part that uses nonlocal resources.

In the “encoder” stage, we need to capture the signal into the quantum memories, which involves a light-matter interaction Hamiltonian. In the naive approach, we could use two-level atoms with ground-excited state encoding, $|g\rangle$, $|e\rangle$, where the energy difference corresponds to that of the photon. If we were to place such an ensemble of excited atoms in a cavity, the atoms will undergo optical decay that can introduce errors or take the state outside the code space. To circumvent this, we use STIRAP which allows us to coherently couple the incoming light into a nonradiative state of an atom. Unlike the naive approach, we do not need to match the frequency of the signal with the atomic transition, providing more bandwidth and flexibility. The state is then imprinted onto a QEC code.

The model.—We model the incoming signal as a weak thermal state [19] that has been multiplexed into frequency bands narrow enough for interferometry. First, consider the case where at most a single photon arrives on the two sites ($\epsilon \ll 1$). For higher photon numbers see Supplemental Material [20]. We can describe the optical state by the density matrix

$$\rho_\star \approx (1 - \epsilon)|\text{vac}, \text{vac}\rangle\langle\text{vac}, \text{vac}|_{AB} + \epsilon\left(\frac{1 + \gamma}{2}\right)|\psi_+^\phi\rangle\langle\psi_+^\phi| + \epsilon\left(\frac{1 - \gamma}{2}\right)|\psi_-^\phi\rangle\langle\psi_-^\phi|, \quad (1)$$

where $|\psi_\pm^\phi\rangle = (|1_p\rangle_A|\text{vac}\rangle_B \pm e^{i\phi}|\text{vac}\rangle_A|1_p\rangle_B)/\sqrt{2}$. Here, the subscript p denotes a photon Fock state of the corresponding photon number.

The parameters of interest are ϕ and γ , where $\phi \in [0, 2\pi)$ is related to the location of the sources, and $\gamma \in [0, 1]$ is proportional to the Fourier transform of the intensity distribution via the van Cittert-Zernike theorem [19]. Optimally estimating ϕ and γ provides complete information of the source distribution [39]. See Supplemental

Material [20] for a review of the QFI [40–48]. Here, we consider a two-mode state for simplicity; this easily extends to multimode, broadband operation by incorporating the time and frequency-multiplexed encoding [5,49]. Our entanglement cost is the same as those in Refs. [5,49] if we use their efficient time-bin encoding. Memoryless schemes similar to Ref. [18] have an entanglement cost scaling as $1/\epsilon$, whereas ours and those of Refs. [5,49] scale as $\log(1/\epsilon)$.

The novel steps introduced in this Letter include (1) transferring the stellar photon modes to atomic states via the STIRAP method, (2) the Bell measurement that encodes the stellar photon into a QEC code, and (3) the quantitative advantage afforded by QEC.

Stimulated Raman adiabatic passage.—STIRAP is inherently robust to parameter errors and resilient to certain types of noise, emerging as a popular tool in quantum information. It is immune to loss through spontaneous emission, and robust against small variations of experimental conditions, e.g., laser intensity and pulse timing [17]. It allows the complete transfer of population along a three-level chain $|0\rangle_R \rightarrow |e\rangle \rightarrow |1\rangle_R$ [Fig. 2(b)] from an initially populated state $|0\rangle_R$ to a target state $|1\rangle_R$ via a light-matter interaction Hamiltonian. We depict our setup in Fig. 2: (a) inside a cavity, we use three systems. We denote the blue array as the register. The blue array is initialized in a code space of a QEC code encoding a single logical qubit, spanned by its logical codewords $|0_L\rangle$ and $|1_L\rangle$. We also need ancilla qubit 1 (green atom with gradient fill), and ancilla atom 2 (red atom with check pattern). Note the three types of matter qubits could consist of different electronic sublevels of the same species of atom if desired.

Panel (b) depicts the energy levels of ancilla atom 2. This atom has three energy levels: the excited state $|e\rangle$, and two ground states, $|0\rangle_R$ and $|1\rangle_R$ that we have assumed degenerate, though this is not essential. The energy

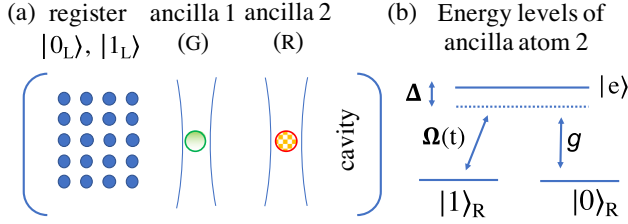


FIG. 2. Cavity-assisted coherent single-photon transfer. (a) A system of qubits has logical states $|0_L\rangle, |1_L\rangle$; ancillary qubit 1 is initially prepared into a Bell state with the register, $1/\sqrt{2}(|0_L0_G\rangle + |1_L1_G\rangle)$; ancilla 2 is used in the STIRAP interaction to interact with the star photon. (b) Energy levels of the ancilla atom 2 used for the STIRAP interaction.

difference between $|0\rangle_R$ and $|e\rangle$ is ω_0 . Ancilla atom 2 is optically trapped. The cavity coupling between $|0\rangle_R$ and $|e\rangle$ is denoted g , which is a fixed parameter that depends on the properties of the atom and the cavity; the time-dependent Rabi frequency on the transition $|1\rangle_R$ to $|e\rangle$ is denoted $\Omega(t)$. The parameter $\Omega(t)$ is tunable via changing the intensity of another laser, which has frequency ω_L , and has detuning Δ from ω_0 .

Defining n to be the number of photons in the cavity, the STIRAP Hamiltonian is

$$H_{\text{STIRAP}}(t) = \omega_0|e\rangle\langle e| + \omega_c a^\dagger a + \Omega(t)e^{-i\omega_L t}|e\rangle\langle 1|_R + \Omega(t)^* e^{i\omega_L t}|1\rangle_R\langle e| + g a|0\rangle_R\langle e| + g^* a^\dagger|e\rangle\langle 0|_R. \quad (2)$$

In the rotating wave approximation, in the basis $\{|1_R, n-1\rangle, |e, n-1\rangle, |0_R, n\rangle\}$, the interaction Hamiltonian can be written as a direct sum,

$$H_I(t) = \bigoplus_n H^{(n)}(t), \quad H^{(n)}(t) = \begin{pmatrix} 0 & \Omega(t)^* & 0 \\ \Omega(t) & -\Delta & g\sqrt{n} \\ 0 & g^*\sqrt{n} & 0 \end{pmatrix}. \quad (3)$$

Here, $\Delta = \omega_L - \omega_0$ is the energy difference between the laser and the transition energy and itself can be a function of time. One of the eigenstates of $H^{(n)}(t)$ has a zero eigenvalue, $H^{(n)}(t)|\psi_0(t)\rangle = 0$, where $|\psi_0(t)\rangle = c(-r(t)|1\rangle_R|n-1\rangle + |0\rangle_R|n\rangle)$, $r(t) = [g\sqrt{n}/\Omega(t)]$, and c is a normalization factor.

If $|\Omega(t=0)| \gg |g|$, then $|\psi_0(t)\rangle \approx |0\rangle_R$, i.e., $|0\rangle_R$ is the zero eigenstate of $H_I(t)$. In our protocol, we initialize the atomic state as $|0\rangle_R$, then we adiabatically tune down $|\Omega(t)|$ such that at the end of the interaction ($t = T$), $|\Omega(T)| \ll |g|$. At this point, the zero eigenstate $|\psi_0(T)\rangle \approx |1\rangle_R$. That is, we have made a controlled spin population transfer from $|0\rangle_R$ to $|1\rangle_R$ depending on the presence of the photon. If the photon is absent, $|0\rangle_R|\text{vac}\rangle$ stays as $|0\rangle_R|\text{vac}\rangle$.

The joint state of the atom-photon evolves as $\rho(T) = U_I(T)\rho(0)U_I^\dagger(T)$, $U_I(T) = \mathcal{T}\{\int_0^T \exp(-iH_I t)dt\}$, where $\mathcal{T}\{\cdot\}$ is the time-ordering operator. Since we stay in the 0 eigenvalue of $H(t)$ for all time there is no dynamical phase accumulated. This is what makes STIRAP robust against timing errors. In Supplemental Material [20], we discuss STIRAP in greater detail and show an explicit pulse that can complete the transfer while minimally populating $|e\rangle\langle e|$ (see also Refs. [50–59]).

The encoder.—Suppose we now prepare the register and the green ancilla (here the subscript G denotes green) in the Bell state

$$|\Phi_0\rangle = \frac{1}{\sqrt{2}}(|0_L\rangle|0_G\rangle + |1_L\rangle|1_G\rangle). \quad (4)$$

Now, the red ancilla is initially prepared in state $|0\rangle_R$, so our setup is in state $|\Psi_0\rangle = |\Phi_0\rangle \otimes |0\rangle_R$. Suppose Alice and Bob each have a copy of $|\Psi_0\rangle$, and they perform STIRAP individually [Fig. 1(iii)]. They share a single photon from the star $(1/\sqrt{2})(|1_p\rangle_A|\text{vac}\rangle_B \pm e^{i\phi}|\text{vac}\rangle_A|1_p\rangle_B)$. In the presence of the photon, the STIRAP interaction transforms $|0\rangle_R \rightarrow |1\rangle_R$, and the phase relationship in the photon is preserved. This means that the state of the red ancillae (on Alice and Bob's sites) is now

$$\frac{1}{\sqrt{2}}(|1_R, 0_R\rangle_{AB} \pm e^{i\phi}|0_R, 1_R\rangle_{AB}). \quad (5)$$

Performing a Bell measurement on the red and green ancillae teleports the state onto the registers. After the Pauli operator correction dependent on the measurement outcome, the state of the registers between Alice and Bob becomes an entangled state, and the entanglement arises entirely from the starlight photon.

Since the starlight state is mixed, after the encoding, the density matrix shared between Alice and Bob is

$$\rho_{AB} \approx (1 - \epsilon)|0_L0_L\rangle\langle 0_L0_L|_{AB} + \epsilon\left(\frac{1+\gamma}{2}\right)|\psi_{+,L}^\phi\rangle\langle\psi_{+,L}^\phi| + \epsilon\left(\frac{1-\gamma}{2}\right)|\psi_{-,L}^\phi\rangle\langle\psi_{-,L}^\phi| + O(\epsilon^2), \quad (6)$$

where $|\psi_{\pm,L}^\phi\rangle = (|0_L, 1_L\rangle \pm e^{i\phi}|1_L, 0_L\rangle)/\sqrt{2}$.

The states $|\psi_{\pm,L}^\phi\rangle$ are orthogonal to $|0_L0_L\rangle$ and $|1_L1_L\rangle$, and therefore can be distinguished via a parity measurement [5]. We can introduce additional preshared logical Bell pairs $|\Phi^\pm\rangle = (|0_L, 0_L\rangle \pm |1_L, 1_L\rangle)/\sqrt{2}$, which can be prepared by injecting a two-qubit Bell pair into Alice and Bob's QEC code by state injection [60]. The quality of the logical Bell pairs can be guaranteed by using distillation protocols [38]. Introducing additional preshared logical Bell pairs $|\Phi^\pm\rangle = (|0_L, 0_L\rangle \pm |1_L, 1_L\rangle)/\sqrt{2}$, logical CZ

gates between the memory qubits in ρ_{AB} and $|\Phi^+\rangle$ can project out the vacuum:

$$\begin{aligned} \rho_{AB} \otimes |\Phi^+\rangle \xrightarrow{2 \times \text{CZ}} & |0_L, 0_L\rangle \langle 0_L, 0_L|_{AB} \otimes |\Phi^+\rangle \langle \Phi^+| \\ & + \epsilon \left(\frac{1+\gamma}{2} \right) |\psi_{+,L}^\phi\rangle \langle \psi_{+,L}^\phi| \otimes |\Phi^-\rangle \langle \Phi^-| \\ & + \epsilon \left(\frac{1-\gamma}{2} \right) |\psi_{-,L}^\phi\rangle \langle \psi_{-,L}^\phi| \otimes |\Phi^-\rangle \langle \Phi^-|. \end{aligned} \quad (7)$$

It suffices for Alice and Bob to perform local measurements to determine if the logical Bell pair is $|\Phi^+\rangle$ or $|\Phi^-\rangle$. For instance, Alice and Bob would both measure in the eigenbasis of the logical X operator, and accept only the odd parity outcome. This odd parity outcome corresponds to a projection onto the state $|\Phi^-\rangle$, which reveals that a star photon has been captured. This method extends to accommodate multiple photon events (Supplemental Material [20]).

After projecting out the vacuum, we can use local measurements to extract ϕ and γ . The QFI for ϕ is $\gamma^2 \epsilon$, and the QFI for γ is $\epsilon/(1-\gamma^2)$. Local measurements are sufficient to saturate the quantum Cramer-Rao bound: indeed, projecting onto $(1/\sqrt{2})(|0_L\rangle \pm e^{i\alpha}|1_L\rangle)_A \otimes (1/\sqrt{2})(|0_L\rangle \pm |1_L\rangle)_B$ is optimal, where α is an adjustable phase. Note that γ and ϕ cannot be optimally simultaneously estimated (Supplemental Material [20]). If we want to avoid applying a logical phase gate, we could robustly do this using geometric phases during the STIRAP stage. By changing the relative phase of the pump pulse $\Omega(t)$ and the single atom coupling g dynamically during the sequence, a geometric phase will accumulate depending on the path in parameter space [61].

Quantum error correction.—After STIRAP and the parity measurement, Alice and Bob share the quantum state ρ'_{AB} in Eq. (6), which is entangled over $2n$ qubits (they each hold n). We can calculate the QFI of ρ'_{AB} with respect to the signal that has been encoded with QEC. For an $[[n, k, d]]$ code, n is the number of physical qubits, k is the number of logical qubits encoded, and d is the distance. The distance is the minimum number of physical errors it takes to change one logical codeword into another. Any QEC code with distance d can correct up to $t = \lfloor (d-1)/2 \rfloor$ errors [62], $\lfloor \cdot \rfloor$ indicates the floor function.

The choice of QEC depends on the number of available qubits and the noise model. We illustrate how our QEC scheme performs when a dephasing channel (see Supplemental Material [20] for depolarizing) afflicts each qubit. If n is small, the exact QFI can be calculated. We describe the dephasing channel as

$$\mathcal{E}_{\text{dephase}}[\rho] \rightarrow (1-p)\rho + p\sigma_z \rho \sigma_z^\dagger, \quad (8)$$

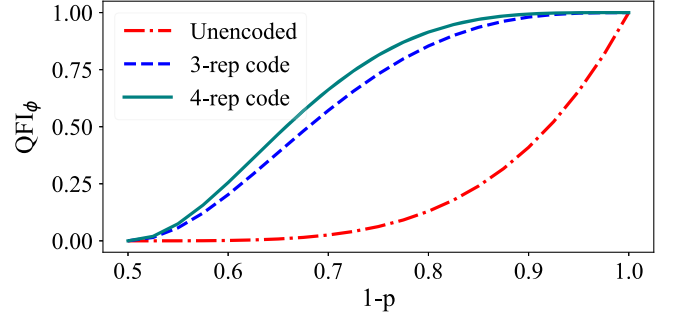


FIG. 3. For $\gamma = 1$, the QFI for ϕ for the dephasing channel, when we use no encoding (red dot-dashed line); the three-repetition code (blue dashed line); and the four-repetition code (teal solid line).

where σ_z is the phase-flip operator. Here, $p = 1/2$ corresponds to the completely dephasing channel.

In Fig. 3 we show the QFI of ϕ per photon as a function p . In most physical systems, dephasing is the dominant noise type. The unprotected case which does not use QEC codes has a QFI of $(1-2p)^4$, which drops off quickly even when p is small. A simple quantum repetition code provides a significant advantage over the unprotected case for all values of dephasing. The logical states of the repetition codes are $|0_L\rangle = |+\rangle^{\otimes n}$ and $|1_L\rangle = |-\rangle^{\otimes n}$, $|\pm\rangle = (|0\rangle + |1\rangle)/\sqrt{2}$; and as n increases, the state becomes more resilient. In the limit of large n , the curve will approach a step function where the QFI is preserved up to $p < 0.5$. This is evident from the Chernoff bound (below) because the phase-flip distance of the repetition code is n .

In Fig. 4 we show the QFI of γ per photon. Note γ is a parameter associated with a nonunitary process, and behaves differently from ϕ : the QFI can be preserved despite more than $(d-1)/2$ errors occurring. Surprisingly, if $\phi = 0$, the repetition code preserves its QFI perfectly. There are two cases leading to this phenomenon: if there are less than n phase errors, the state is put onto a correctable

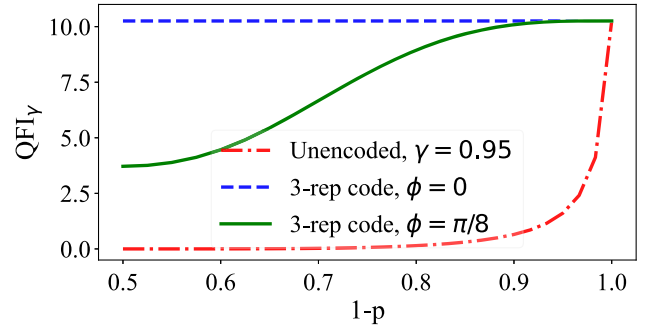


FIG. 4. For $\gamma = 0.95$, the QFI for γ of the dephasing channel, when no encoding is used (red dot-dashed line), and the three-repetition code, when $\phi = 0$ (blue dashed line), and when $\phi = \pi/8$ (green solid line).

subspace, and the corresponding normalized state has the same QFI as the original. When $2n$ phase-flip errors occur, the logical states $(|0_L\rangle|1_L\rangle \pm |1_L\rangle|0_L\rangle)/\sqrt{2}$ are eigenvectors of these errors with eigenvalues ± 1 : the state is invariant under the noise channel.

To understand the behavior of large quantum codes, now let us consider any noise model that introduces error on each qubit independently with probability p . Let ϵ_{fail} denote the probability of having an uncorrectable error, where ϵ_{fail} is at most the probability of having at least $d/2$ errors. Using the Chernoff-Hoeffding bound for Bernoulli random variables [63], whenever $p < d/(2n)$, we have [64,65]

$$\epsilon_{\text{fail}} \leq e^{-D(p||d/2n)n}, \quad (9)$$

where $D(x||y) = x \ln(x/y) + (1-x) \ln[(1-x)/(1-y)]$ denotes the Kullback-Leibler divergence. Note that ϵ_{fail} vanishes exponentially in n for small enough p . For large QEC codes, $d/(2n)$ asymptotes to a positive constant. By the quantum Gilbert-Varshamov bound [66–69], we know that if we use random QEC codes, we can have d/n approaching 0.1893 for large n . Hence, for our scheme, such QEC codes can tolerate noise afflicting up to 9.4% of the qubits while preserving the QFI. See Supplemental Material [20] for further discussions.

Discussions and conclusions.—We have proposed a general framework for applying QEC to an imaging task, where the experimenter did not prepare the probe. Although we cannot illuminate our objects for astronomical imaging, we can nonetheless perform superresolution imaging beyond the diffraction limit [44,70–72]. From this perspective, our Letter complements the active research area of superresolution imaging [70,73–80].

We have entered the stage where tens—soon hundreds—of qubits are becoming available. Much effort has focused on using noisy intermediate-scale quantum (NISQ) [81] devices to demonstrate capabilities that surpass classical computers. We have proposed an application for a NISQ device for imaging. For the dominant noise type—dephasing—we show that a significant advantage can be gained even with a simple repetition code, and we can tolerate error rates up to 50%. For noise types (even adversarial) that corrupt up to a certain fraction of the qubits we find the threshold of 9.4% for which the QFI can be preserved. This threshold is significantly less stringent than that required for quantum computation.

Z. H. is supported by a Sydney Quantum Academy Postdoctoral Fellowship, and thanks Jonathan P. Dowling for inspiring this line of research. We thank Thomas Volz for his insightful discussions. G. K. B. acknowledges support from the Australian Research Council Centre of Excellence for Engineered Quantum Systems (Grant No. CE170100009). Y. O. is supported by the Quantum Engineering Programme Grant No. NRF2021-QEP2-01-P06,

and also in part by NUS startup grants (No. R-263-000-E32-133 and No. R-263-000-E32-731), and the National Research Foundation, Prime Minister’s Office, Singapore and the Ministry of Education, Singapore under the Research Centres of Excellence program.

*zixin.huang@mq.edu.au

†gavin.brennen@mq.edu.au

‡oyingkai@gmail.com

- [1] V. Giovannetti, S. Lloyd, and L. Maccone, *Phys. Rev. Lett.* **96**, 010401 (2006).
- [2] V. Giovannetti, S. Lloyd, and L. Maccone, *Nat. Photonics* **5**, 222 (2011).
- [3] J. W. Lichtman and J.-A. Conchello, *Nat. Methods* **2**, 910 (2005).
- [4] C. A. Casacio, L. S. Madsen, A. Terrasson, M. Waleed, K. Barnscheidt, B. Hage, M. A. Taylor, and W. P. Bowen, *Nature (London)* **594**, 201 (2021).
- [5] E. T. Khabiboulline, J. Borregaard, K. De Greve, and M. D. Lukin, *Phys. Rev. Lett.* **123**, 070504 (2019).
- [6] B. M. Terhal, *Rev. Mod. Phys.* **87**, 307 (2015).
- [7] S. Zhou, M. Zhang, J. Preskill, and L. Jiang, *Nat. Commun.* **9**, 1 (2018).
- [8] R. Demkowicz-Dobrzański, J. Czajkowski, and P. Sekatski, *Phys. Rev. X* **7**, 041009 (2017).
- [9] Z. Huang, C. Macchiavello, and L. Maccone, *Phys. Rev. A* **94**, 012101 (2016).
- [10] N. Shettell, W. J. Munro, D. Markham, and K. Nemoto, *New J. Phys.* **23**, 043038 (2021).
- [11] E. M. Kessler, I. Lovchinsky, A. O. Sushkov, and M. D. Lukin, *Phys. Rev. Lett.* **112**, 150802 (2014).
- [12] W. Dür, M. Skotiniotis, F. Fröwis, and B. Kraus, *Phys. Rev. Lett.* **112**, 080801 (2014).
- [13] T. Uden, P. Balasubramanian, D. Louzon, Y. Vinkler, M. B. Plenio, M. Markham, D. Twitchen, A. Stacey, I. Lovchinsky, A. O. Sushkov, M. D. Lukin, A. Retzker, B. Naydenov, L. P. McGuinness, and F. Jelezko, *Phys. Rev. Lett.* **116**, 230502 (2016).
- [14] D. Layden, S. Zhou, P. Cappellaro, and L. Jiang, *Phys. Rev. Lett.* **122**, 040502 (2019).
- [15] Y. Ouyang, N. Shettell, and D. Markham, *IEEE Trans. Inf. Theory* **68**, 1809 (2022).
- [16] Y. Ouyang and N. Rengaswamy, [arXiv:2007.02859](https://arxiv.org/abs/2007.02859).
- [17] N. V. Vitanov, A. A. Rangelov, B. W. Shore, and K. Bergmann, *Rev. Mod. Phys.* **89**, 015006 (2017).
- [18] D. Gottesman, T. Jennewein, and S. Croke, *Phys. Rev. Lett.* **109**, 070503 (2012).
- [19] L. Mandel and E. Wolf, *Optical Coherence and Quantum Optics* (Cambridge University Press, Cambridge, England, 1995).
- [20] See Supplemental Material at <http://link.aps.org/supplemental/10.1103/PhysRevLett.129.210502> for a review of quantum metrology, which includes Refs. [21–38].
- [21] D. W. Leung, M. A. Nielsen, I. L. Chuang, and Y. Yamamoto, *Phys. Rev. A* **56**, 2567 (1997).
- [22] Y. Ouyang, *Phys. Rev. A* **90**, 062317 (2014).
- [23] D. K. Tuckett, S. D. Bartlett, and S. T. Flammia, *Phys. Rev. Lett.* **120**, 050505 (2018).

- [24] A. Ashikhmin, S. Litsyn, and M. A. Tsfasman, *Phys. Rev. A* **63**, 032311 (2001).
- [25] H. Chen, S. Ling, and C. Xing, *IEEE Trans. Inf. Theory* **47**, 2055 (2001).
- [26] Z. Li, L. Xing, and X. Wang, *IEEE Trans. Inf. Theory* **55**, 3821 (2009).
- [27] A. S. Darmawan, B. J. Brown, A. L. Grimsmo, D. K. Tuckett, and S. Puri, *PRX Quantum* **2**, 030345 (2021).
- [28] A. G. Fowler, M. Mariantoni, J. M. Martinis, and A. N. Cleland, *Phys. Rev. A* **86**, 032324 (2012).
- [29] Y. Wu, S. Kolkowitz, S. Puri, and J. D. Thompson, *Nat. Commun.* **13**, 4657 (2022).
- [30] P. Pantelev and G. Kalachev, in *Proceedings of the 54th Annual ACM SIGACT Symposium on Theory of Computing* (2022), pp. 375–388.
- [31] Y. Ouyang, in *Proceedings of the 2021 IEEE International Symposium on Information Theory (ISIT)* (2021), pp. 1499–1503, [10.1109/ISIT45174.2021.9518078](https://doi.org/10.1109/ISIT45174.2021.9518078).
- [32] T. Shibayama and M. Hagiwara, *2021 IEEE International Symposium on Information Theory (ISIT)* (2021), p. 1493, [10.1109/ISIT45174.2021.9517870](https://doi.org/10.1109/ISIT45174.2021.9517870).
- [33] A. Nakayama and M. Hagiwara, *IEICE Commun. Express* **9**, 100 (2020).
- [34] T. Shibayama and Y. Ouyang, in *Proceedings of the 2021 IEEE Information Theory Workshop (ITW)* (IEEE, New York, 2021), pp. 1–6.
- [35] P. Baireuther, M. D. Caio, B. Criger, C. W. Beenakker, and T. E. O'Brien, *New J. Phys.* **21**, 013003 (2019).
- [36] R. Chao and B. W. Reichardt, *PRX Quantum* **1**, 010302 (2020).
- [37] A. Z. Goldberg and D. F. V. James, *Phys. Rev. A* **100**, 042332 (2019).
- [38] E. T. Campbell, B. M. Terhal, and C. Vuillot, *Nature (London)* **549**, 172 (2017).
- [39] M. E. Pearce, E. T. Campbell, and P. Kok, *Quantum* **1**, 21 (2017).
- [40] S. L. Braunstein and C. M. Caves, *Phys. Rev. Lett.* **72**, 3439 (1994).
- [41] I. Afnan, R. Banerjee, S. L. Braunstein, I. Brevik, C. M. Caves, B. Chakraborty, E. Fischbach, L. Lindblom, G. Milburn, S. Odintsov *et al.*, *Ann. Phys. (N.Y.)* **247**, 447 (1996).
- [42] M. G. Paris, *Int. J. Quantum. Inform.* **07**, 125 (2009).
- [43] S. Ragy, M. Jarzyna, and R. Demkowicz-Dobrzański, *Phys. Rev. A* **94**, 052108 (2016).
- [44] C. Lupo, Z. Huang, and P. Kok, *Phys. Rev. Lett.* **124**, 080503 (2020).
- [45] D. W. Berry, H. M. Wiseman, and J. K. Breslin, *Phys. Rev. A* **63**, 053804 (2001).
- [46] D. W. Berry and H. M. Wiseman, *Phys. Rev. Lett.* **85**, 5098 (2000).
- [47] Z. Huang, K. R. Motes, P. M. Anisimov, J. P. Dowling, and D. W. Berry, *Phys. Rev. A* **95**, 053837 (2017).
- [48] M. Jarzyna and R. Demkowicz-Dobrzański, *Phys. Rev. Lett.* **110**, 240405 (2013).
- [49] E. T. Khabiboulline, J. Borregaard, K. De Greve, and M. D. Lukin, *Phys. Rev. A* **100**, 022316 (2019).
- [50] G. S. Vasilev, A. Kuhn, and N. V. Vitanov, *Phys. Rev. A* **80**, 013417 (2009).
- [51] B. W. Shore, *Adv. Opt. Photon.* **9**, 563 (2017).
- [52] T. Cubel, B. K. Teo, V. S. Malinovsky, J. R. Guest, A. Reinhard, B. Knuffman, P. R. Berman, and G. Raithe, *Phys. Rev. A* **72**, 023405 (2005).
- [53] M. Saffman, T. G. Walker, and K. Mølmer, *Rev. Mod. Phys.* **82**, 2313 (2010).
- [54] N. Timoney, I. Baumgart, M. Johanning, A. Varón, M. B. Plenio, A. Retzker, and C. Wunderlich, *Nature (London)* **476**, 185 (2011).
- [55] S. C. Webster, S. Weidt, K. Lake, J. J. McLoughlin, and W. K. Hensinger, *Phys. Rev. Lett.* **111**, 140501 (2013).
- [56] T. S. Koh, S. Coppersmith, and M. Friesen, *Proc. Natl. Acad. Sci. U.S.A.* **110**, 19695 (2013).
- [57] J.-Q. You and F. Nori, *Nature (London)* **474**, 589 (2011).
- [58] S. Garcia, F. Ferri, J. Reichel, and R. Long, *Opt. Express* **28**, 15515 (2020).
- [59] P. Jessen, D. Haycock, G. Klose, G. Smith, I. Deutsch, and G. Brennen, *Quantum Inf. Comput.* **1**, 20 (2001).
- [60] X. Zhou, D. W. Leung, and I. L. Chuang, *Phys. Rev. A* **62**, 052316 (2000).
- [61] D. Møller, L. B. Madsen, and K. Mølmer, *Phys. Rev. A* **75**, 062302 (2007).
- [62] J. Roffe, *Contemp. Phys.* **60**, 226 (2019).
- [63] W. Hoeffding, *The Collected Works of Wassily Hoeffding* (Springer, New York, 1994), [10.1007/978-1-4612-0865-5_26](https://doi.org/10.1007/978-1-4612-0865-5_26).
- [64] H. Chernoff *et al.*, *Ann. Math. Stat.* **23**, 493 (1952).
- [65] M. Okamoto, *Ann. Inst. Stat. Math.* **10**, 29 (1959).
- [66] K. Feng and Z. Ma, *IEEE Trans. Inf. Theory* **50**, 3323 (2004).
- [67] Y. Ma, *J. Math. Anal. Appl.* **340**, 550 (2008).
- [68] L. Jin and C. Xing, in *Proceedings of the IEEE International Symposium on Information Theory Proceedings (ISIT)* (2011), pp. 455–458.
- [69] Y. Ouyang, *IEEE Trans. Inf. Theory* **60**, 3117 (2014).
- [70] M. Tsang, *Contemp. Phys.* **60**, 279 (2019).
- [71] R. Nair and M. Tsang, *Phys. Rev. Lett.* **117**, 190801 (2016).
- [72] Z. Huang and C. Lupo, *Phys. Rev. Lett.* **127**, 130502 (2021).
- [73] Z. Huang, C. Lupo, and P. Kok, *PRX Quantum* **2**, 030303 (2021).
- [74] M. P. Backlund, Y. Shechtman, and R. L. Walsworth, *Phys. Rev. Lett.* **121**, 023904 (2018).
- [75] Z. Yu and S. Prasad, *Phys. Rev. Lett.* **121**, 180504 (2018).
- [76] C. Napoli, S. Piano, R. Leach, G. Adesso, and T. Tufarelli, *Phys. Rev. Lett.* **122**, 140505 (2019).
- [77] W.-K. Tham, H. Ferretti, and A. M. Steinberg, *Phys. Rev. Lett.* **118**, 070801 (2017).
- [78] M. Parniak, S. Borówka, K. Boroszko, W. Wasilewski, K. Banaszek, and R. Demkowicz-Dobrzański, *Phys. Rev. Lett.* **121**, 250503 (2018).
- [79] S. A. Wadood, K. Liang, Y. Zhou *et al.*, *Opt. Express* **29**, 22034 (2021).
- [80] Y. Zhou, J. Yang, J. D. Hassett, S. M. H. Rafsanjani, M. Mirhosseini, A. N. Vamivakas, A. N. Jordan, Z. Shi, and R. W. Boyd, *Optica* **6**, 534 (2019).
- [81] J. Preskill, *Quantum* **2**, 79 (2018).